JOURNAL OF CHEMICAL EDUCATION

Cite This: J. Chem. Educ. 2019, 96, 1752−1759

Laboratory Experiment

pubs.acs.org/jchemeduc

An Undergraduate Experiment To Explore Cu(II) Coordination Environment in Multihistidine Compounds through Electron Spin Resonance Spectroscopy

Eugene P. Wagner,* Kai C. Gronborg, Shreya Ghosh, and Sunil Saxena*

Department of Chemistry, University of Pittsburgh, Pittsburgh, Pennsylvania 15260, United States

Supporting Information

ABSTRACT: Electron spin resonance (ESR) or electron paramagnetic resonance (EPR) spectroscopy is an incisive technique for the characterization of paramagnetic centers in inorganic, bioinorganic, and organic molecules and materials. These measurements are enabled with the help of paramagnetic species, such as organic free radicals and ions, electronically excited states, and metal−ligand compounds, some of which with biological importance. In this experiment, analogues of histidine−copper coordination compounds are investigated to show students how ESR line shapes depend on the complexed copper ion electronic structure as well as how the spectral features elucidate the coordination environment of copper. These coordinated compounds play an important role in metal ion coordination in proteins and peptides. The experiment has two parts. First, three copper−imidazole complexes that mimic copper−histidine compounds in the human body are synthesized. Second, the ESR spectrum of each complex is obtained at 77 K from frozen chloroform/methanol and acetonitrile/methanol matrixes and used to elucidate the ligand arrangement of the Cu^{2+} ion and the effect on the unpaired electron density.

KEYWORDS: *Upper-Division Undergraduate, Biochemistry, Physical Chemistry, Hands-On Learning/Manipulatives, Biophysical Chemistry, EPR/ESR Spectroscopy, Laboratory Equipment/Apparatus, Laboratory Instruction, Organometallics*

Electron spin resonance (ESR) or electron paramagnetic resonance (EPR) spectroscopy is an invaluable technique with applications that span all branches of natural sciences. ESR detects species with unpaired electron spins and is increasingly used to probe the structure and function of spin labeled macromolecules. Pulsed ESR techniques can measure distances between two unpaired electrons on the order of 2−16 nm with angstrom level resolution.[1−11] The lack of size limitation, high sensitivity, and ability to conduct experiments under various conditions like micelles, vesicles, cells, and nanodiscs add to its advantage. Moreover, the rare presence of other unpaired electrons, besides the ones placed as a probe, minimizes unwanted background signal in the ESR signal. ESR can also be used to monitor radical formation in chemical reactions and in degradation processes. As a biophysical tool, ESR has been extensively used for probing structure and dynamics of proteins and nucleic acids[1,2,12−25] as well as protein−nucleic acid complexes.[26−31] Hence, ESR plays an important role in advancing the field of biophysics. The wide-reaching applications and unique information about electron density and chemical structure provided by ESR make it an important magnetic resonance spectroscopy technique to be covered in the undergraduate chemistry curriculum. Several ESR laboratory experiments designed for upper level undergraduate courses have been reported in this *Journal*. Some focus on kinetic studies,[32−34] others focus on coordinated compound structure,[35−41] and two show direct application to bioinorganic chemistry.[42,43] The experiment described here also has a direct application to biochemistry while providing learning opportunities on the correlation of electron density to changes in metal−ligand structure. In this designed laboratory experiment, ESR spectra are used to elucidate the coordination environment of Cu(II).[44] It is important to discriminate between the different coordination modes in order to better understand the biological role in several metal−protein complexes.[45−47] For example, changes in Cu(II) coordination play a crucial role in the formation of aggregates of the protein amyloid-β, which is responsible for Alzheimer's disease.[44,48−50]

In this experiment, three Cu^{2+} complexes with different numbers of imidazole ligand are first synthesized and then investigated to compare systematic changes in ESR spectra, specifically the **g**-tensor ($g_{\parallel}$) and hyperfine coupling ($A_{\parallel}$) values. This experiment is appropriate for biochemistry, inorganic chemistry, and physical chemistry undergraduate laboratory courses. The experiment can be completed by two-person lab groups in a 4 h lab period, provided that the fundamentals of ESR spectroscopy are covered in a prelab lecture, activity, or assignment. The experiment is appropriate for any upper level laboratory course that has physical chemistry lecture as a prerequisite or co-requisite.

BACKGROUND

Copper Biochemistry

Copper is an essential element for all aerobic organisms. It plays an important role as a cofactor in a number of important enzymes. Copper cycles between cuprous and cupric states by exchanging electrons, and this property has made it an essential component for catalyzing a wide variety of biochemical processes. In other systems, such as amyloid-β (Aβ), prion,

Received: March 4, 2019
Revised: May 30, 2019
Published: June 19, 2019

DOI: 10.1021/acs.jchemed.9b00190
J. Chem. Educ. 2019, 96, 1752−1759

and α-synuclein, modified copper homeostasis can lead to generation of toxic aggregates resulting in several neurodegenerative diseases, such as Alzheimer's and Parkinson's diseases.[51−58]

Histidine is one of the strongest metal ion coordinators in proteins. Histidine contains an imidazole ligand with two nitrogen atoms to which Cu^{2+} can bind. Copper-containing proteins often have binding sites with irregular geometries containing one or more histidine ligands.[59−61] In amyloidogenic proteins, small changes in coordination affect the rate of aggregation, aggregate morphology, and other chemical mechanisms.[44,51,54,55,62,63] For all these reasons, significant efforts by researchers have been put into understanding the structural details of metal coordination in order to understand the chemical basis of function.

ESR

The following basics of ESR spectroscopy are presented in an abridged manner, and coverage is limited to those aspects specifically required to complete the described experiment. For a more complete discussion of ESR fundamentals and theory, readers are encouraged to review the texts by Weil and Bolton,[64] and by Lindon.[65]

A continuous wave (CW) ESR instrument is a commonly used experimental method. A CW-ESR spectrum is obtained by placing a sample with unpaired electrons in a microwave field of constant frequency (ν) and sweeping the external magnetic field (B). When the energy of the applied microwave radiation ($h\nu$) matches the energy separation between the spin-states, absorption occurs. The transitions in a CW experiment can be better understood by examining the dominant terms in the electron spin Hamiltonian (eq 1).

$$\hat{H} = |\beta_e|\vec{B}\cdot\vec{\vec{g}}\cdot\hat{S} + \sum_{i=1}^{k}\hat{S}\cdot\vec{\vec{A}}\cdot\hat{I}_i \tag{1}$$

The two terms on the right-hand side of the equation are the electron Zeeman interaction and the hyperfine interaction. Here, $\vec{B}$ is the magnetic field vector, and $\hat{S}$ and $\hat{I}$ are the electron and nuclear spin angular momentum operators, respectively; β_e is the electron Bohr magneton, $\vec{\vec{g}}$ is the electron **g**-tensor, and $\vec{\vec{A}}$ is the hyperfine tensor. Both $\vec{\vec{g}}$ and $\vec{\vec{A}}$ are second-order tensors, and further details on the nature of these values are provided in the Supporting Information. The Hamiltonian in eq 1 ignores nuclear Zeeman and nuclear quadrupole interactions, since they are comparatively small and do not significantly affect the CW spectrum. Similarly, for simplicity, we consider only the dominant terms that typically affect CW line shape, i.e., the electron Zeeman and the hyperfine interaction with the Cu(II) nuclei.

The electron Zeeman interaction is the interaction between the electron spin and the external magnetic field. The electron spin also experiences a magnetic field induced by the interaction of the orbital angular momentum with the applied magnetic field and from spin−orbit coupling.[66] This induced magnetic field depends on the shape of the orbital in which the unpaired electron is delocalized, and on the orientation of the molecule in the magnetic field. On the other hand, the dominant hyperfine interaction is the interaction between the unpaired electron spin and the nuclear spin of Cu^{2+}. Additional information and details on these fundamental aspects of ESR are provided in the Supporting Information. The energy level diagram for Cu^{2+} is shown in Figure 1. The Cu^{2+} ion has an

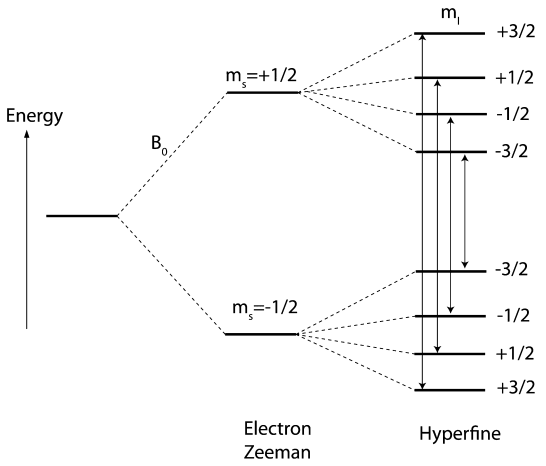

Figure 1. Energy level diagram of Cu^{2+}.

electron spin of 1/2 (m_S = +1/2, −1/2) and a nuclear spin of 3/2 (m_I = +3/2, + 1/2, −1/2, −3/2), where m_S and m_I are the quantum numbers for the z-components of electron spin angular momentum and nuclear spin angular momentum operators, respectively. Hence, following the selection rules of $\Delta m_S = \pm 1$ and $\Delta m_I = 0$, four hyperfine transitions are observed.

At low temperature and in a frozen matrix, the Cu^{2+} CW ESR spectrum provides relevant information about the coordination environment of the metal ion. First, consider the case of the **g**-tensor only. We restrict our discussion to the case of axially symmetric tensors. In a sample, all the molecules are randomly oriented as illustrated in Figure 2B. The resonance occurs at

$$h\nu = g(\theta)\beta_e B \tag{2}$$

where h is Planck's constant and $g(\theta)$ is given as[67]

$$g(\theta) = \sqrt{g_\perp^2 \sin^2\theta + g_\parallel^2 \cos^2\theta} \tag{3}$$

The subscripts $\perp$ and $\parallel$ refer, respectively, to the xx/yy and zz molecular axes (Figure 2).

Since the sample is frozen, all θ angles will be captured (Figure 2B), giving a range of resonant magnetic fields. However, statistically there are more molecules whose xx,yy-axes will be aligned with the magnetic field than the zz-axis. Hence, the intensity of the spectrum increases sinusoidally from when the zz-axis is parallel to the magnetic field ($\theta = 0°$) to when the xx,yy plane is parallel to the field ($\theta = 90°$) (trace I of Figure 2C). Trace II of Figure 2C shows the first derivative of the absorption spectrum, which is how a CW-ESR spectrum is recorded for instrumental reasons, which is beyond the scope of this paper.[64]

The hyperfine interaction leads to splitting of the line shape shown in Figures 1 and 2C. Thus, for a particular θ, the resonance condition is

$$h\nu = g(\theta)\beta_e B + A(\theta)m_I \tag{4}$$

where $A(\theta)$ is given as[67]

$$A(\theta) = \sqrt{\frac{A_\perp^2 g_\perp^4 \sin^2\theta + A_\parallel^2 g_\parallel^4 \cos^2\theta}{g_\perp^2 \sin^2\theta + g_\parallel^2 \cos^2\theta}} \tag{5}$$

DOI: 10.1021/acs.jchemed.9b00190
J. Chem. Educ. 2019, 96, 1752−1759

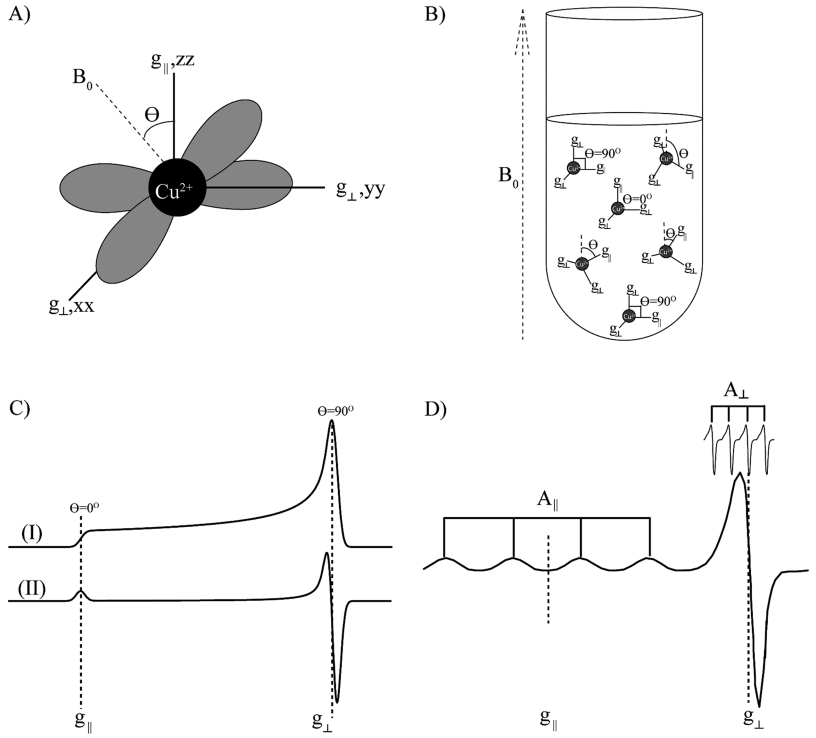

Figure 2. (A) Unpaired electron in Cu^{2+} present in the d_{x2-y2} orbital. Type II Cu^{2+} shows axial symmetry whereby $g_{xx} = g_{yy} = g_{\perp}$ and $g_{zz} = g_{\parallel}$. The angle θ is the angle between the applied magnetic field and the molecular zz-axis. (B) A sample of randomly oriented molecules with random θ values. (C) For a sample with random orientations, there will be higher probability for the molecules to be at $\theta = 90°$than $\theta = 0°$. As such, the intensity corresponding to $\theta = 90°$ will be the highest as shown in trace I. Trace II shows the first derivative of the absorption spectrum, as seen in CW-ESR. D) CW-ESR spectrum of Cu^{2+} at low temperature.

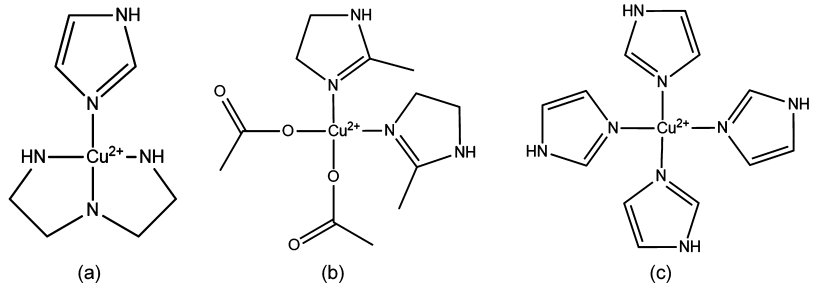

Figure 3. Equatorial coordination of Cu^{2+} in the model complexes: (a) dienimidazolecopper(II) diperchlorate (1-imidazole), (b) bis(2-methylimidazole)copper(II) diacetate (2-imidazole), and (c) tetrakisimidazolecopper(II) sulfate (4-imidazole). The axial water ligands are not shown.

The resultant CW-ESR spectrum is shown in Figure 2D. The $g_{\parallel}$ and $A_{\parallel}$ are usually better resolved and, hence, are used to determine the coordination environment of Cu^{2+}.

At low temperature (~77 K), the Cu^{2+} solution is frozen, and all possible orientations of θ are sampled. Cu^{2+} has one unpaired electron in the d_{x2-y2} orbital and thus shows axial symmetry, which leads to $g_{xx} = g_{yy} \equiv g_{\perp}$ and $g_{zz} \equiv g_{\parallel}$ (Figure 2A). Similarly, the components of the **A**-tensor for Cu^{2+} are $A_{xx} = A_{yy} \equiv A_{\perp}$ and $A_{zz} \equiv A_{\parallel}$.

The coordination environment of Cu^{2+}, a d^9 system, often forms a distorted octahedral geometry (axial elongation) with ligands, due to Jahn–Teller distortion. This means that the four ligands present in the equatorial plane are strongly bonded to the Cu^{2+} ion, while the two axial ligands, perpendicular to the equatorial plane, have longer bond lengths and thus are weakly coordinated to Cu^{2+}. As a result, the interaction between the unpaired electron and the axial ligands is relatively weak with regard to affecting the ESR signal. Conversely, directly coordinated equatorial ligands have a stronger interaction with the unpaired electron. The electron withdrawing strength of the equatorial ligands around the copper ion affects how unpaired electron density diffuses in the d orbital, which in turn affects the $g_{\parallel}$ value. Similarly, the $A_{\parallel}$ value is also dependent on the directly coordinated ligands. Refer to the Supporting Information for a more detailed discussion on $g_{\parallel}$ and $A_{\parallel}$.

■ EXPERIMENTAL PROCEDURE

For this experiment, analogues of three copper–histidine complexes, dienimidazolecopper(II) diperchlorate (1-imidazole), bis(2-methylimidazole)copper(II) diacetate (2-imidazole), and tetrakisimidazolecopper(II) sulfate (4-imidazole), are used to investigate and identify ligand arrangements (Figure 3). The complexes are first synthesized and then

DOI: 10.1021/acs.jchemed.9b00190
J. Chem. Educ. 2019, 96, 1752–1759

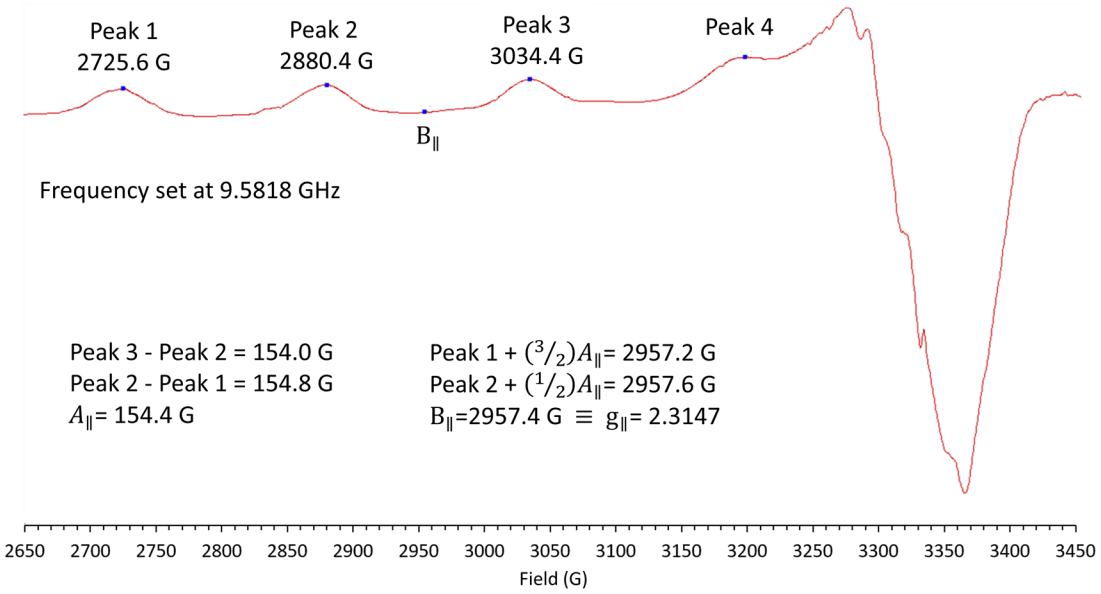

Figure 4. ESR spectrum for bis(2-methylimidazole) copper(II) diacetate (2-imidazole). While the fourth peak for $A_{\|}$ is partially resolved in this spectrum, it is typically obscured by the $A_{\perp}$ peaks and not used to determine $A_{\|}$ and $g_{\|}$. The $B_{\|}$ value is converted to the $g_{\|}$ value using either eq 6 or eq 7.

analyzed through ESR to identify ligand arrangements and changes to the unpaired electron density. The synthesis methods are based on published work with modifications to simplify and expedite the process for students.[44,68−70] The 1-imidazole is prepared at room temperature by mixing equivalent mole amounts of copper(II) perchlorate hexahydrate, diethylenetriamine, and imidazole in a methanol/acetonitrile solvent. The 2-imidazole requires heating a 2:1 mol ratio of 2-methylimidazole to anhydrous copper(II) acetate in a chloroform/methanol solution for 45 min at 50 °C. The 4-imidazole requires mixing a 4:1 mol ratio of imidazole to copper(II) sulfate pentahydrate in water. All compound solutions are diluted with a 25% glycerol/methanol solution to concentrations that provide good resolution and intensity of ESR absorption peaks. 2,2-Diphenyl-1-picrylhydrazyl organic radical (DPPH) is used as a standard for determining the *g*-factor value of an electron free from any orbital momentum coupling. A materials list and detailed procedure for synthesis are available in the Supporting Information.

While the complexes must be analyzed in the frozen state, DPPH can be analyzed at room temperature. Obtaining the DPPH spectrum first allows students to become familiar with ESR instrument operation without the complication of a low temperature study. It also allows them to confirm the free-electron *g*-factor value and be certain of proper field center setting of the spectrometer, instrument operation, and *g*-factor calculations. DPPH has an unpaired electron diffusely distributed throughout the molecule. As a result, the coupling constants are very small, and the spectrum is typically viewed as one peak. The complexes are analyzed at liquid nitrogen temperature (~77 K) through the use of a finger Dewar inserted into the ESR cavity. A field sweep width of approximately 700 G on an X-band ESR spectrometer is necessary to observe the entire spectrum.

HAZARDS

Standard laboratory safety procedures were followed, including wearing goggles and gloves. The synthesis and sample preparation were performed in fume hoods. Methanol, acetonitrile, chloroform, and diethylenetriamine liquids are flammable and toxic if inhaled or ingested. The organic solids DPPH, imidazole, and 2-methylimidazole, as well as the copper(II) sulfate pentahydrate, copper(II) acetate, and copper(II) perchlorate hexahydrate salts, can cause skin and eye irritation and are toxic if ingested. In addition, copper(II) perchlorate hexahydrate is a strong oxidizing solid. While this salt is relatively stable and safe to use in the teaching laboratory, explicit instructions for safe handling practices should be provided to the students. All of these chemicals, especially the copper(II) perchlorate hexahydrate, should be kept in tightly sealed containers in a dry and well-ventilated space. Liquid nitrogen is a cryogenic fluid that can cause severe freezing of skin and asphyxiation. Appropriate personal protection equipment was used when handling liquid nitrogen in a well-ventilated area.

RESULTS

Figure 4 shows a typical spectrum acquired for the 2-imidazole complex. Three of the peaks used to determine $A_{\|}$ are well-resolved. The last peak (highest field) is partially obscured by $A_{\perp}$ peaks. Therefore, the $A_{\|}$ value needed for analysis is obtained by averaging the field difference between the first and second peaks and second and third peaks. The $B_{\|}$ field position, correlating to $g_{\|}$, can be found by adding $(3A_{\|}/2)$ to the first (most low field) peak or $(A_{\|}/2)$ to the second peak. The $B_{\|}$ field value is converted to a corresponding unitless $g_{\|}$ value through eq 6, where $h\nu$ is the microwave radiation energy and β_e is the electron Bohr magneton.

$$\Delta E = h\nu = g_{\|}\beta_e B_{\|} \tag{6}$$

If obtaining a precise instrument frequency value is not possible, as is the case with an older Varian ESR, DPPH can be

DOI: 10.1021/acs.jchemed.9b00190
J. Chem. Educ. 2019, 96, 1752−1759

added to each sample and the ratio of the DPPH field absorption peak to the $B_{\|}$ field value of the complex can be used to determine $g_{\|}$ through eq 7:

$$g_{\|,\text{complex}} = g_{\text{DPPH}} \frac{B_{\text{DPPH}}}{B_{\|,\text{complex}}} \quad (7)$$

While modeling the ESR spectrum to obtain these values would be best, students have consistently obtained values very similar to modeling data using this simplified analysis method. However, the relative comparison of the $A_{\|}$ and $g_{\|}$ among the three complexes is more important than absolute accuracy of each of these values. The hyperfine values, given here in Gauss, can also be converted into units of energy such as MHz or cm^{-1} (see Supporting Information).

As shown in Table 1, the changes in the Cu^{2+} coordination environment are directly reflected in the $A_{\|}$ and $g_{\|}$ values.[71]

Table 1. Measured Values for $A_{\|}$ and $g_{\|}$[a]

Compound	$g_{\|}$	$A_{\|}$ (G)
1-Imidazole	2.216	192.2
2-Imidazole	2.315	154.4
4-Imidazole	2.269	180.4

[a]The DPPH reference molecule is isotropic with g = 2.0037.

These trends are similar to that noted in the literature.[44,71] Note that there are two nitrogen and two oxygen atoms (referred to as 2N2O) that coordinate to Cu(II) in the 2-imidazole complex whereas four nitrogen atoms (referred to as 4N) are bonded to Cu(II) for the 1- and 4- imidazole complexes (Figure 3). Such a difference in the local coordination environment led to changes in $A_{\|}$ and $g_{\|}$ values. The $g_{\|}$ values are strongly dependent on the coupling between the spin and the orbital angular momentum. See the Supporting Information for a detailed discussion. A greater spin−orbit coupling (SOC) leads to a greater deviation in the g-value from the free-electron g-factor value. When Cu^{2+} is coordinated to nitrogen, the covalency of the bond increases, thereby decreasing the SOC and consequently decreasing $g_{\|}$. Thus, as the Cu^{2+} coordination is 4N for the 1- and 4-imidazole complexes (Figure 3), the $g_{\|}$ values are lower than that of the 2-imidazole complex which has a 2N2O direct coordination.

An inverse relation of the $A_{\|}$ and $g_{\|}$ is observed in this data. Increase in covalency of the metal−ligand bond leads to greater delocalization of the electron density. As a result, the interaction between the electron and nuclear spin increases, thereby increasing the $A_{\|}$ value (cf. eq S8 in Supporting Information). Thus, the electron density at the Cu^{2+} nucleus decreases on going from a 4N to a 2N2O coordination, as the covalency is greater for nitrogen than oxygen. Consequently, the 2-imidazole complex (2N2O) has a lower $A_{\|}$ value than the 1- or 4-imidaole complex (4N).

Often there are distinct features in the $A_{\perp}$ region which are due to a superhyperfine interaction[44] between the electron spin of Cu^{2+} with the nuclear spin of the directly coordinated nitrogen. The features due to this interaction become more distinct as the number of directly coordinated imidazole rings increases.

IMPACT ON LEARNING

This experiment has been performed by 105 students working in groups of two for the past three semesters in our physical chemistry laboratory I course required for all chemistry majors. Additionally, some chemical engineering majors take this course as an elective. The lab consists of seven experiments conducted in a round robin fashion. There are up to 12 students in a laboratory section and four to five different experiments are scheduled each week with students working in pairs. Student groups not scheduled to perform an experiment in a specific week are expected to work on data analysis and reports for experiments conducted in prior weeks. There are no prelab lectures for the experiments. Instead, students are expected to complete a reading assignment specific to the particular experiment, review the lab manual procedures, and complete a prelab assignment before conducting the experiment. During the laboratory session, instructors facilitate students with experiment logistics and procedure as well as answer questions about the fundamental aspects of the technique and related chemistry. The relatively small number of students in a lab section allows for more personalized and frequent interaction with the instructor. For example, instructors are able to discuss ESR fundamentals, such as Zeeman splitting, g-factor, and hyperfine interaction, with students as these particular aspects and questions arise during the lab session.

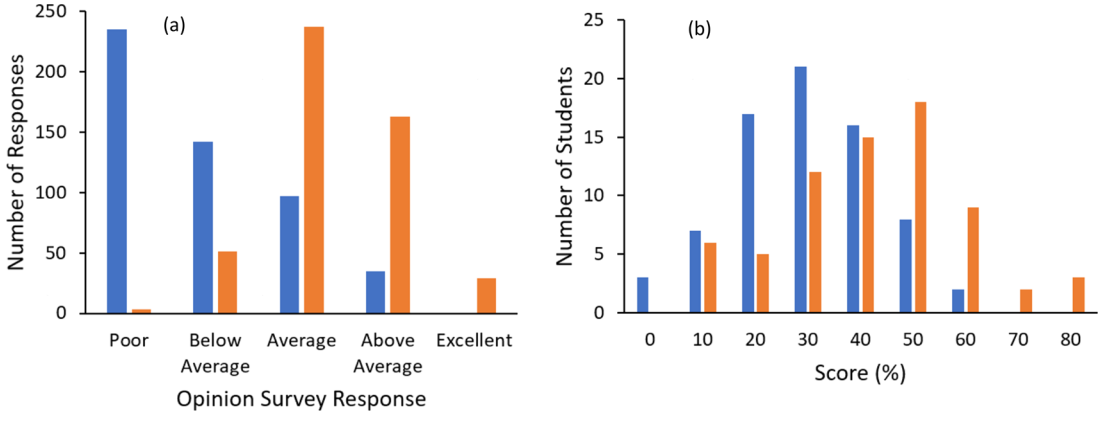

Figure 5. Cumulative data over three semesters (N = 105). The pre (blue) and post (orange) results of (a) the opinion survey and (b) the multiple-choice ESR knowledge assessment. The opinion survey shows a significant increase in the mean Likert scale value of 1.87−3.34 (P < 0.05). Performance on the formal assessment of ESR knowledge also significantly increased from 29.7% to 42.0% (P < 0.05).

DOI: 10.1021/acs.jchemed.9b00190
J. Chem. Educ. 2019, 96, 1752−1759

The impact of this ESR experiment on both perceived and formally assessed knowledge was quantified through two pre- and postassessments. The opinion survey included seven questions asking students to rank their knowledge on various ESR topics compared to their peers on a Likert scale (1 = poor to 5 = excellent). A 10-question multiple choice quiz was used to objectively evaluate their ESR knowledge. Both assessments were administered on the first class meeting of the semester in order to obtain baseline data for student opinion and knowledge of ESR before any formal exposure to the subject or experiment. Once all of the groups had completed the ESR experiment and report, the same assessments were administered again near the end of the semester to determine both the impact and changes in opinion and knowledge of ESR fundamentals. Both assessments are provided in the Supporting Information.

Opinion survey data indicated that, before the lab, most students ranked their ESR knowledge at an average of 1.87 correlating to below average to poor compared to the knowledge of their peers (Figure 5a). This result shifted to a majority of students ranking their knowledge as being average to above average after completing the lab, with the mean Likert value of 3.34. The multiple-choice assessment on ESR knowledge shows a similar trend as the distribution of scores shifts from an average of 29.7% before conducting the experiment to an average of 42.0% (Figure 5b) after completing the experiment and laboratory report. Both the student opinion survey and the knowledge assessment increases were statistically significant ($P < 0.05$). While the average score on the postsemester knowledge assessment is a concern, it should be noted that this is the only experiment in the laboratory curriculum where the fundamental principles are not covered in the prerequisite physical chemistry lecture course. As such, the first experience students have on the ESR topic is this experiment. Given the situation, students do make adequate gains in learning this complicated topic through the assigned reading, conducting the experiment, and writing the report. Further, they complete their undergraduate education with more understanding and appreciation for ESR spectroscopy than they otherwise would have without this experiment.

CONCLUSION

In this laboratory experiment, students carried out the synthesis of three copper(II) complexes with varying numbers of imidazole ligands. ESR was used to analyze the coordination of the synthesized compounds from the $g_{\|}$ and $A_{\|}$ values obtained from the ESR spectrum. The data was used to draw conclusions pertaining to the ligand effects on the metal unpaired electron density and coordination environment. Students gained knowledge and confidence in their abilities pertaining to ESR theory, technique, instrumentation, and application. While the impact on learning assessment results indicates a significant increase in understanding of ESR fundamental concepts and knowledge, there is still room for growth. Incorporating additional exposure to ESR prior to conducting this experiment through the physical chemistry lecture course or formal prelab lecture could provide students with a solid theoretical background that this experiment could build upon. Regardless of whether the fundamentals of ESR are covered in a formal lecture course, students still gain an insight into the interdisciplinary applications of ESR, a better understanding of ESR, and an appreciation for the instrumental technique through the laboratory experiment.

ASSOCIATED CONTENT

Supporting Information

The Supporting Information is available on the ACS Publications website at DOI: 10.1021/acs.jchemed.9b00190.

Student laboratory instructions (PDF, DOCX)

Notes for instructors (PDF, DOCX)

Student opinion survey and knowledge quiz used for learning assessment (PDF, DOCX)

AUTHOR INFORMATION

Corresponding Authors

*E-mail: ewagner@pitt.edu.
*E-mail: sksaxena@pitt.edu.

ORCID

Eugene P. Wagner: 0000-0002-8615-1517
Kai C. Gronborg: 0000-0001-9726-2311
Sunil Saxena: 0000-0001-9098-6114

Notes

The authors declare no competing financial interest.

ACKNOWLEDGMENTS

This work was supported in part by grants from National Science Foundation (NSF MCB-1613007 and NSF MRI-1725678) to S.S. Dr. Ishara Silva is thanked for several discussions. S.G. thanks the Pittsburgh Quantum Institute for the semester fellowship.

REFERENCES

(1) Borbat, P. P.; Freed, J. H. Pulse Dipolar ESR: Distance Measurements. In *Structural Information from Spin-Labels and Intrinsic Paramagnetic Centers in the Biosciences. Structure and Bonding*; Timmel, C. R., Harmer, J. R., Eds.; Springer: New York, 2012; pp 1−82.

(2) Jeschke, G. DEER Distance Measurements on Proteins. *Annu. Rev. Phys. Chem.* **2012**, *63*, 419−446.

(3) Milov, A. D.; Maryasov, A. G.; Tsvetkov, Y. D. Pulsed Electron Double Resonance (PELDOR) and Its Applications in Free-Radicals Research. *Appl. Magn. Reson.* **1998**, *15*, 107−143.

(4) Saxena, S.; Freed, J. H. Double Quantum Two-Dimensional Fourier Transform Electron Spin Resonance: Distance Measurements. *Chem. Phys. Lett.* **1996**, *251* (1−2), 102−110.

(5) Pannier, M.; Veit, S.; Godt, A.; Jeschke, G.; Spiess, H. Dead-Time Free Measurement of Dipole-Dipole Interactions between Electron Spins. *J. Magn. Reson.* **2000**, *142* (2), 331−340.

(6) Milikisyants, S.; Scarpelli, F.; Finiguerra, M. G.; Ubbink, M.; Huber, M. A Pulsed EPR Method to Determine Distances between Paramagnetic Centers with Strong Spectral Anisotropy and Radicals: The Dead-Time Free RIDME Sequence. *J. Magn. Reson.* **2009**, *201* (1), 48−56.

(7) Jeschke, G.; Pannier, M.; Godt, A.; Spiess, H. W. Dipolar Spectroscopy and Spin Alignment in Electron Paramagnetic Resonance. *Chem. Phys. Lett.* **2000**, *331* (2−4), 243−252.

(8) Kulik, L. V.; Dzuba, S. A.; Grigoryev, I. A.; Tsvetkov, Y. D. Electron Dipole-dipole Interaction in ESEEM of Nitroxide Biradicals. *Chem. Phys. Lett.* **2001**, *343* (3−4), 315−324.

(9) Becker, J. S.; Saxena, S. Double Quantum Coherence Electron Spin Resonance on Coupled Cu(II)-Cu(II) Electron Spins. *Chem. Phys. Lett.* **2005**, *414* (1−3), 248−252.

(10) Bonora, M.; Becker, J.; Saxena, S. Suppression of Electron Spin-Echo Envelope Modulation Peaks in Double Quantum Coherence Electron Spin Resonance. *J. Magn. Reson.* **2004**, *170* (2), 278−283.

(11) Ruthstein, S.; Ji, M.; Shin, B.; Saxena, S. A Simple Double Quantum Coherence ESR Sequence That Minimizes Nuclear

DOI: 10.1021/acs.jchemed.9b00190
J. Chem. Educ. 2019, 96, 1752−1759

Modulations in Cu2+-Ion Based Distance Measurements. *J. Magn. Reson.* **2015**, *257*, 45−50.
(12) Goldfarb, D. Gd3+ Spin Labeling for Distance Measurements by Pulse EPR Spectrscopy. *Phys. Chem. Chem. Phys.* **2014**, *16*, 9685−9699.
(13) Ji, M.; Ruthstein, S.; Saxena, S. Paramagnetic Metal Ions in Pulsed ESR Distance Distribution Measurements. *Acc. Chem. Res.* **2014**, *47*, 688−695.
(14) Yang, Z.; Ji, M.; Cunningham, T. F.; Saxena, S. Cu(II) as an ESR Probe of Protein Structure and Function. *Methods Enzymol.* **2015**, *563*, 459.
(15) Hubbell, W. L.; Lopez, C. J.; Altenbach, C.; Yang, Z. Technological Advances in Site-Directed Spin Labeling of Proteins. *Curr. Opin. Struct. Biol.* **2013**, *23*, 725−733.
(16) Schiemann, O.; Prisner, T. F. Long-Range Distance Determinations in Biomacromolecules by EPR Spectroscopy. *Q. Rev. Biophys.* **2007**, *40* (1), 1.
(17) Berliner, L. J.; Eaton, S. S.; Eaton, G. R. *Distance Measurements in Biological Systems by EPR*; Springer Science and Business Media, 2006.
(18) Reginsson, G. W.; Schiemann, O. Pulsed Electron-electron Double Resonance: Beyond Nanometre Distance Measurements on Biomacromolecules. *Biochem. J.* **2011**, *434* (3), 353−363.
(19) Cafiso, D. S. Identifying and Quantitating Conformational Exchange in Membrane Proteins Using Site-Directed Spin Labeling. *Acc. Chem. Res.* **2014**, *47* (10), 3102−3109.
(20) Glaenzer, J.; Peter, M. F.; Hagelueken, G. Studying Structure and Function of Membrane Proteins with PELDOR/DEER Spectroscopy - The Crystallographers' Perspective. *Methods* **2018**, *147*, 163−175.
(21) Lawless, M. J.; Sarver, J.; Saxena, S. Nucleotide-Independent copper(II)-Based Distance Measurements in DNA by Pulsed ESR Spectroscopy. *Angew. Chem., Int. Ed.* **2017**, *56*, 2115−2117.
(22) Marko, A.; Denysenkov, V.; Margraf, D.; Cekan, P.; Schiemann, O.; Sigurdsson, S. T.; Prisner, T. F. Conformational Flexibility of DNA. *J. Am. Chem. Soc.* **2011**, *133*, 13375−13379.
(23) Schiemann, O.; Piton, N.; Mu, Y.; Stock, G.; Engels, J. W.; Prisner, T. F. A PELDOR-Based Nanometer Distance Ruler for Oligonucleotides. *J. Am. Chem. Soc.* **2004**, *126* (18), 5722−5729.
(24) Endeward, B.; Marko, A.; Denysenkov, V. P.; Sigurdsson, S. T.; Prisner, T. F. Advanced EPR Methods for Studying Conformational Dynamics of Nucleic Acids. *Methods Enzymol.* **2015**, *564*, 403−425.
(25) Milikisiyants, S.; Wang, S.; Munro, R. A.; Donohue, M.; Ward, M. E.; Bolton, D.; Brown, L. S.; Smirnova, T. I.; Ladizhansky, V.; Smirnov, A. I. Oligomeric Structure of Anabaena Sensory Rhodopsin in a Lipid Bilayer Environment by Combining Solid-State NMR and Long-Range DEER Constraints. *J. Mol. Biol.* **2017**, *429* (12), 1903−1920.
(26) Yang, Z.; Kurpiewski, M. R.; Ji, M.; Townsend, J. E.; Mehta, P.; Jen-Jacobson, L.; Saxena, S. ESR Spectroscopy Identifies Inhibitory Cu2+ Sites in a DNA-Modifying Enzyme to Reveal Determinants of Catalytic Specificity. *Proc. Natl. Acad. Sci. U. S. A.* **2012**, *109* (17), E993−1000.
(27) Ji, M.; Tan, L.; Jen-Jacobson, L.; Saxena, S. Insights into Copper Coordination in the EcoRI-DNA Complex by ESR Spectroscopy. *Mol. Phys.* **2014**, *112* (24), 3173−3182.
(28) Grytz, C. M.; Marko, A.; Cekan, P.; Sigurdsson, S. T.; Prisner, T. F. Flexibility and Conformation of the Cocaine Aptamer Studied by PELDOR. *Phys. Chem. Chem. Phys.* **2016**, *18*, 2993−3002.
(29) Nguyen, P. H; Popova, A. M; Hideg, K.; Qin, P. Z A Nucleotide-Independent Cyclic Nitroxide Label for Monitoring Segmental Motions in Nucleic Acids. *BMC Biophys.* **2015**, *8*, 6−14.
(30) Stone, K. M.; Townsend, J. E.; Sarver, J.; Sapienza, P. J.; Saxena, S.; Jen-Jacobson, L. Electron Spin Resonance Shows Common Structural Features for Different Classes of Eco RI-DNA Complexes. *Angew. Chem.* **2008**, *120* (52), 10346−10348.
(31) Reginsson, G. W.; Shelke, S. A.; Rouillon, C.; White, M. F.; Sigurdsson, S. T.; Schiemann, O. Protein-Induced Changes in DNA Structure and Dynamics Observed with Noncovalent Site-Directed Spin Labeling and PELDOR. *Nucleic Acids Res.* **2013**, *41* (1), e11−e11.
(32) Schmallegger, M.; Gescheidt, G. Antioxidant Activity of Beer: An EPR Experiment for an Undergraduate Physical-Chemistry Laboratory. *J. Chem. Educ.* **2018**, *95* (11), 2013−2016.
(33) Signorella, S.; Rizzotto, M.; Mulero, M.; Garcia, S.; Frascaroli, M.; Sala, L. F. Easy Experiments for Detection of Chromium Intermediates. *J. Chem. Educ.* **1992**, *69* (7), 578.
(34) Pickering, M. Radical Recombination Kinetics: An Experiment in Physical Organic Chemistry. *J. Chem. Educ.* **1980**, *57* (11), 833.
(35) Butera, R. A.; Waldeck, D. H. An EPR Experiment for the Undergraduate Physical Chemistry Laboratory. *J. Chem. Educ.* **2000**, *77* (11), 1489.
(36) Basu, P. Use of EPR Spectroscopy in Elucidating Electronic Structures of Paramagnetic Transition Metal Complexes. *J. Chem. Educ.* **2001**, *78* (5), 666.
(37) Garribba, E.; Micera, G. The Determination of the Geometry of Cu(II) Complexes: An EPR Spectroscopy Experiment. *J. Chem. Educ.* **2006**, *83* (8), 1229.
(38) Abell, T. N.; McCarrick, R. M.; Bretz, S. L.; Tierney, D. L. Trispyrazolylborate Complexes: An Advanced Synthesis Experiment Using Paramagnetic NMR, Variable-Temperature NMR, and EPR Spectroscopies. *J. Chem. Educ.* **2017**, *94* (12), 1960−1964.
(39) Sojka, Z.; Stopa, G. Analysis of the Isotropic EPR Spectrum of K3[Cr(CN)5NO]: An Inorganic Chemistry Laboratory Experiment. *J. Chem. Educ.* **1993**, *70* (8), 675.
(40) Berry, D. E.; Hicks, R. G.; Gilroy, J. B. The Chemistry of Formazan Dyes. Synthesis and Characterization of a Stable Verdazyl Radical and a Related Boron-Containing Heterocycle. *J. Chem. Educ.* **2009**, *86* (1), 76.
(41) Ugone, V.; Garribba, E.; Micera, G.; Sanna, D. Equilibrium between Different Coordination Geometries in Oxidovanadium(IV) Complexes. *J. Chem. Educ.* **2015**, *92* (6), 1098−1102.
(42) Linenberger, K.; Bretz, S. L.; Crowder, M. W.; McCarrick, R.; Lorigan, G. A.; Tierney, D. L. What Is the True Color of Fresh Meat? A Biophysical Undergraduate Laboratory Experiment Investigating the Effects of Ligand Binding on Myoglobin Using Optical, EPR, and NMR Spectroscopy. *J. Chem. Educ.* **2011**, *88* (2), 223−225.
(43) Vincent, J. B.; Woski, S. A. Cytochrome c: A Biochemistry Laboratory Course. *J. Chem. Educ.* **2005**, *82* (8), 1211.
(44) Silva, K. I.; Michael, B. C.; Geib, S. J.; Saxena, S. ESEEM Analysis of Multi-Histidine Cu(II)-Coordination in Model Complexes, Peptides, and Amyloid-B. *J. Phys. Chem. B* **2014**, *118*, 8935−8944.
(45) McCracken, J.; Peisach, J.; Dooley, D. M. Cu(II) Coordination Chemistry of Amine Oxidases: Pulsed EPR Studies of Histidine Imidazole, Water, and Exogenous Ligand Coordination. *J. Am. Chem. Soc.* **1987**, *109*, 4064−4072.
(46) Lu, J.; Bender, C. J.; McMillin, D. R.; McCracken, J.; Peisach, J.; Severns, J. C. Pulsed EPR Studies of the Type 2 Copper Binding Site in the Mercury Derivative of Laccase. *Biochemistry* **1992**, *31* (27), 6265−6272.
(47) Jiang, F.; McCracken, J.; Peisach, J. Nuclear Quadrupole Interactions in Copper(II)-Diethylenetriamine-Substituted Imidazole Complexes and in Copper(II) Proteins. *J. Am. Chem. Soc.* **1990**, *112*, 9035−9044.
(48) Shin, B.; Saxena, S. Substantial Contribution of the Two Imidazole Rings of the His13-His14 Dyad to Cu(II) Binding in Amyloid-β(1−16) at Physiological pH and Its Significance. *J. Phys. Chem. A* **2011**, *115* (34), 9590−9602.
(49) Hernandez-Guzman, J.; Sun, L.; Mehta, A. K.; Dong, J.; Lynn, D. G.; Warncke, K. Copper(II)-Bis-Histidine Coordination Structure in a Fibrillar Amyloid B-Peptide Fragment and Model Complexes Revealed by Electron Spin Echo Envelope Modulation Spectroscopy. *ChemBioChem* **2013**, *14*, 1762−1771.
(50) Gunderson, W. A.; Hernández-Guzmán, J.; Karr, J. W.; Sun, L.; Szalai, V. A.; Warncke, K. Local Structure and Global Patterning of Cu2+ Binding in Fibrillar Amyloid-β [Aβ(1−40)] Protein. *J. Am. Chem. Soc.* **2012**, *134* (44), 18330−18337.

DOI: 10.1021/acs.jchemed.9b00190
J. Chem. Educ. 2019, 96, 1752−1759

(51) Faller, P.; Hureau, C. Bioinorganic Chemistry of Copper and Zinc Ions Coordinated to Amyloid-β Peptide. *Dalt. Trans.* **2009**, *0* (7), 1080−1094.
(52) Bush, A. I. The Metallobiology of Alzheimer's Disease. *Trends Neurosci.* **2003**, *26* (4), 207−214.
(53) Talmard, C.; Guilloreau, L.; Coppel, Y.; Mazarguil, H.; Faller, P. Amyloid-Beta Peptide Forms Monomeric Complexes With CuII and ZnII Prior to Aggregation. *ChemBioChem* **2007**, *8* (2), 163−165.
(54) Miller, L. M.; Wang, Q.; Telivala, T. P.; Smith, R. J.; Lanzirotti, A.; Miklossy, J. Synchrotron-Based Infrared and X-Ray Imaging Shows Focalized Accumulation of Cu and Zn Co-Localized with β-Amyloid Deposits in Alzheimer's Disease. *J. Struct. Biol.* **2006**, *155* (1), 30−37.
(55) Jun, S.; Saxena, S. The Aggregated State of Amyloid-β Peptide In Vitro Depends on Cu2+ Ion Concentration. *Angew. Chem.* **2007**, *119* (21), 4033−4035.
(56) Jun, S.; Gillespie, J. R.; Shin, B.; Saxena, S. The Second Cu(II)-Binding Site in a Proton-Rich Environment Interferes with the Aggregation of Amyloid-β(1−40) into Amyloid Fibrils. *Biochemistry* **2009**, *48* (45), 10724−10732.
(57) Dudzik, C. G.; Walter, E. D.; Millhauser, G. L. Coordination Features and Affinity of the Cu2+ Site in the α-Synuclein Protein of Parkinson's Disease. *Biochemistry* **2011**, *50* (11), 1771−1777.
(58) Dudzik, C. G.; Walter, E. D.; Abrams, B. S.; Jurica, M. S.; Millhauser, G. L. Coordination of Copper to the Membrane-Bound Form of α-Synuclein. *Biochemistry* **2013**, *52* (1), 53−60.
(59) Solomon, E. I.; Hare, J. W.; Dooley, D. M.; Dawson, J. H.; Stephens, P. J.; Gray, H. B. Spectroscopic Studies of Stellacyanin, Plastocyanin, and Azurin. Electronic Structure of the Blue Copper Sites. *J. Am. Chem. Soc.* **1980**, *102* (1), 168−178.
(60) De Rienzo, F.; Gabdoulline, R.R.; Menziani, M. C.; Wade, R.C. Blue Copper Proteins: A Comparative Analysis of Their Molecular Interaction. *Protein Sci.* **2000**, *9* (8), 1439−1454.
(61) Ryde, U.; Olsson, M. H. M.; Pierloot, K. The Structure and Function of Blue Copper Proteins. *Theor. Comput. Chem.* **2001**, *9*, 1−55.
(62) Viles, J. H. Metal Ions and Amyloid Fiber Formation in Neurodegenerative Diseases. Copper, Zinc and Iron in Alzheimer's, Parkinson's and Prion Diseases. *Coord. Chem. Rev.* **2012**, *256* (19−20), 2271−2284.
(63) Syme, C. D.; Nadal, R. C.; Rigby, S. E. J.; Viles, J. H. Copper Binding to the Amyloid-B (AB) Peptide Associated with Alzheimer's Disease. *J. Biol. Chem.* **2004**, *279*, 18169−18177.
(64) Weil, J. A.; Bolton, J. R. *Electron Paramagnetic Resonance: Elementary Theory and Practical Applications*; Wiley-Interscience, 2007.
(65) Lindon, J. C.; Tranter, G. E.; Koppenaal, D. W. *Encyclopedia of Spectroscopy and Spectrometry*; Elsevier, 2016.
(66) Slichter, C. P. *Principles of Magnetic Resonance*; Springer Series in Solid-State Sciences; Springer: Berlin, 1990; Vol. *1*. DOI: 10.1007/978-3-662-09441-9.
(67) Raymond Hagen, W. *Biomolecular EPR Spectroscopy*; CRC Press: Boca Raton, FL, 2008. DOI: 10.1201/9781420059588.
(68) Fransson, G.; Lundberg, B. K. S. Metal Complexes with Mixed Ligands - The Crystal Structure of Tetrakisimidazole Cu(II) Sulphate. *Acta Chem. Scand.* **1972**, *26*, 3969−3976.
(69) Abuhijleh, A. L.; Woods, C.; Ahmed, I. Y. Synthesis and Molecular Structure of Monomeric copper(II) Acetates with 2-Methylimidazole and 1,2-Dimethylimidazole. *Inorg. Chim. Acta* **1991**, *190* (1), 11−17.
(70) Sato, M.; Nagae, S.; Ohmae, K.; Nakaya, J.; Miki, K.; Kasai, N. Preparation and Crystal Structure of an Imidazolate-Bridged Polynuclear Complex [{Cu(im)(dien)} N][ClO_4] N (Dien = Diethylenetriamine), and Its Properties in Dimethyl Sulfoxide Solution. *J. Chem. Soc., Dalton Trans.* **1986**, *0* (9), 1949.
(71) Peisach, J.; Blumberg, W. E. Structural Implications Derived from the Analysis of Electron Paramagnetic Resonance Spectra of Natural and Artificial Copper Proteins. *Arch. Biochem. Biophys.* **1974**, *165* (2), 691−708.

DOI: 10.1021/acs.jchemed.9b00190
J. Chem. Educ. 2019, 96, 1752−1759